

Evaluation of the drug-drug interaction potential of treosulfan using a physiologically-based pharmacokinetic modelling approach

Stephan Schaller¹  | Frederico S. Martins¹  | Pavel Balazki¹  | Sonja Böhm²  |
Joachim Baumgart²  | Ralf A. Hilger³ | Dietrich W. Beelen³  |
Claudia Hemmelmann² | Arne Ring^{2,4} 

¹esqLABS GmbH, Saterland, Germany

²medac Gesellschaft für klinische Spezialpräparate mbH, Wedel, Germany

³West German Cancer Centre, University Hospital Essen, Essen, Germany

⁴Department for Mathematical Statistics and Actuarial Science, University of the Free State, Nelson Mandela Drive, Bloemfontein, South Africa

Correspondence

Stephan Schaller, esqLABS GmbH, Hambierich 34, 26683 Saterland, Germany.
Email: stephan.schaller@esqlabs.com

Funding information

medac GmbH

Aims: The aim of this work is the development of a mechanistic physiologically-based pharmacokinetic (PBPK) model using in vitro to in vivo extrapolation to conduct a drug-drug interaction (DDI) assessment of treosulfan against two cytochrome p450 (CYP) isoenzymes and P-glycoprotein (P-gp) substrates.

Methods: A PBPK model for treosulfan was developed de novo based on literature and unpublished clinical data. The PBPK DDI analysis was conducted using the U.S. Food and Drug Administration (FDA) DDI index drugs (probe substrates) midazolam, omeprazole and digoxin for CYP3A4, CYP2C19 and P-gp, respectively. Qualified and documented PBPK models of the probe substrates have been adopted from an open-source online model database.

Results: The PBPK model for treosulfan, based on both in vitro and in vivo data, was able to predict the plasma concentration-time profiles and exposure levels of treosulfan applied for a standard conditioning treatment. Medium and low potentials for DDI on CYP3A4 (maximum area under the concentration-time curve ratio (AUCR_{max} = 2.23) and CYP2C19 (AUCR_{max} = 1.6) were predicted, respectively, using probe substrates midazolam and omeprazole. Treosulfan was not predicted to cause a DDI on P-gp.

Conclusion: Medicinal products with a narrow therapeutic index (eg, digoxin) that are substrates for CYP3A4, CYP2C19 or P-gp should not be given during treatment with treosulfan. However, considering the comprehensive treosulfan-based conditioning treatment schedule and the respective pharmacokinetic properties of the concomitantly used drugs (eg, half-life), the potential for interaction on all evaluated mechanisms would be low (AUCR < 1.25), if concomitantly administered drugs are dosed either 2 hours before or 8 hours after the 2-hour intravenous infusion of treosulfan.

KEYWORDS

anticancer therapy, drug-drug interaction, inhibitor, modelling and simulation, pharmacokinetics

The authors confirm that there is no principal investigator for this study.

This is an open access article under the terms of the Creative Commons Attribution-NonCommercial-NoDerivs License, which permits use and distribution in any medium, provided the original work is properly cited, the use is non-commercial and no modifications or adaptations are made.

© 2021 medac GmbH. *British Journal of Clinical Pharmacology* published by John Wiley & Sons Ltd on behalf of British Pharmacological Society.

1 | INTRODUCTION

Treosulfan (L-threitol-1,4-bis-methanesulfonate) is a prodrug of a bifunctional alkylating agent with cytotoxic, myeloablative and immunosuppressive properties applied in the treatment of ovarian cancer and conditioning therapy prior to haematopoietic stem cell transplantation.^{1,2} Indication-dependent, it can be administered intravenously or orally in single doses of 3–8 g/m² every 2 weeks or intravenously at higher doses of 10–14 mg/m² on 3 consecutive days. Treosulfan is structurally related to busulfan, from which it differs in two hydroxyl groups, leading to a different mechanism of alkylation.³ Treosulfan is nonenzymatically, pH-dependently converted into its monoepoxide and diepoxide transformation products (2S,3S)-1,2-epoxybutane-3,4-diol 4-methanesulfonate and (2S,3S)-1,2:3,4-diepoxybutane (S,S-EBDM and S,S-DEB, respectively). These mono- and diepoxide transformation products of treosulfan are considered to be the active cytotoxic species and are responsible for DNA alkylation, crosslinking of DNA and proteins, chromosomal aberration, and, finally, subsequent interference with various actions, including genotoxicity and induction of apoptosis.⁴ However, the levels of S,S-DEB in the whole body, including cell nuclei, are expected to be several orders of magnitude lower than that of S,S-EBDM.^{5,6}

Understanding drug-drug interactions (DDIs) is a critical part of the drug development process since a clinically relevant change in the exposure of a co-administered drug can lead to loss of efficacy or, conversely, an adverse drug reaction, depending on the therapeutic window of the victim drug.⁷ The DDI risk becomes important for anti-cancer drugs since these drugs are typically administered close to the maximum tolerated dose.⁸ About 20–30% of all adverse drug reactions have been reported to be caused by DDIs,⁷ contributing to 4% of overall death rates in cancer patients.⁹

The evaluation of potential DDI events is instigated at an early stage in drug discovery with preclinical assessment and characterization using appropriate *in vitro* tools of human systems. Depending on the outcomes of a thorough risk assessment, formal clinical studies may be necessary to address labelling requirements and support prescribing information.⁷ The advances in modelling and simulation approaches (eg, physiologically-based pharmacokinetics [PBPKs]) have enabled a more quantitative perspective to better inform decision-making around DDI risk assessment and mitigation, a strategy that has evolved mainly from the fact that chronic drug therapy and polypharmacy are commonplace in many patient populations.⁷ PBPK models are mathematical models that mechanistically describe the pharmacokinetics (PKs) of xenobiotics based on their physicochemical properties and the physiology of the exposed species. They are typically composed of multiple compartments, each representing a separate organ or tissue, interconnected via transport rate equations representing the circulatory system of the body. Relying on a priori knowledge on partly independent physiological processes integrated within a mechanistic framework, PBPK models allow the prediction and description of absorption, distribution, metabolism, excretion (ADME) properties, and DDI of a drug.^{10–13}

What is already known about this subject

- Treosulfan is a prodrug of a bifunctional alkylating agent with cytotoxic, myeloablative and immunosuppressive properties applied in the treatment of ovarian cancer and conditioning therapy prior to hematopoietic stem cell transplantation.
- Previously conducted detailed *in vitro* studies did not completely exclude potential interactions between high plasma concentrations of treosulfan and CYP3A4, CYP2C19 or P-gp substrates.

What this study adds

- This study is the first physiologically-based pharmacokinetic (PBPK) model developed for treosulfan.
- This work leverages PBPKs to provide drug-drug interaction (DDI) guidance in the patient population under treatment with treosulfan.
- Using the probe substrates midazolam, omeprazole and digoxin, medium and low potentials for DDI on CYP3A4 (AUCR = 2.23) and CYP2C19 (AUCR = 1.6) were predicted, while treosulfan was not assessed as an inhibitor of P-gp (AUCR < 1.25).

The objective of the presented analysis was to conduct a PBPK DDI analysis on CYP3A4, CYP2C19 and P-gp inhibition by treosulfan. The PBPK DDI analysis was conducted using the FDA DDI index drugs (probe substrates) midazolam, omeprazole and digoxin for CYP3A4, CYP2C19 and P-gp, respectively.

2 | METHODS

2.1 | Clinical data

The pharmacokinetic study population (clinical phase III trial MC-FludT.14/L Part I) consisted of 24 patients aged from 43 to 70 years with acute myeloid leukemia (AML) or myelodysplastic syndrome (MDS) who were randomised into the treosulfan arm and received preparative treatment prior to allogeneic hematopoietic stem cell transplantation. Treosulfan concentrations were determined in plasma and urine for the evaluation of pharmacokinetic parameters. The treosulfan plasma levels were measured by 20 blood samples (3 mL of whole blood each, total 60 mL) on day –6 (hours 0 [prior to the infusion]), 2 [immediately after the 2-hour treosulfan infusion], 2.5, 3, 4, 5, 6, 8 and 12 hours after the start of the treosulfan infusion, day –5 (hours 0 [immediately prior to the second treosulfan infusion]), 2 [immediately after the second 2-hour treosulfan infusion] and day –4 (hours 0 [immediately prior to the third treosulfan infusion]),

2 [immediately after the third 2-hour treosulfan infusion], 2.5, 3, 4, 5, 6, 8, 12 and 24 hours after the start of the third treosulfan infusion) (3 mL of whole blood each, total 60 mL). Urine samples were collected from 4-hour fractions of total urine volume collected for 72 hours during the three consecutive treosulfan treatment days (day –6 to day –4). These studies were conducted in accordance with the Declaration of Helsinki and the International Conference on Harmonization/Good Clinical Practice. The final protocol and informed consent form were approved by the institutional review boards at the respective study sites. Informed consent was obtained from all volunteers before any study procedures were conducted.¹⁴

2.2 | Cytochrome P450 inhibition

Six treosulfan concentrations (ranging from 40 to 10 000 μM in water) and human liver microsomes (final concentration 0.25 mg/mL) were pre-incubated each for 30 min in the absence and presence of NADPH or underwent a 0 min pre-incubation¹⁵ (unpublished data). At the end of the pre-incubation period, probe substrates of the respective CYP isoenzymes and NADPH (1 mM) were added (final DMSO concentration 0.05%), and the samples were incubated for 5 min at 37 °C. The time-dependent inhibitors, furafylline (CYP1A2 inhibition), thiotepa (CYP2B6 inhibition), gemfibrozil 1-O- β -glucuronide (CYP2C8 inhibition), tienilic acid, (CYP2C9 inhibition), fluoxetine (CYP2C19 inhibition), paroxetine (CYP2D6 inhibition) and mifepristone (CYP3A4 inhibition) were screened alongside the test compound treosulfan as a positive control. The respective probe substrates were phenacetin, bupropion, paclitaxel, diclofenac, mephenytoin, dextromethorphan and midazolam/testosterone.

A decrease in the formation of the metabolite compared to vehicle control was used to calculate an IC_{50} value (test compound concentration that produces 50% inhibition; Supporting Information Figures S13 and S14) for each experimental condition. The fold shift in IC_{50} was calculated using the following equation:

$$\text{fold shift} = \frac{\text{IC}_{50}(\text{minus})}{\text{IC}_{50}(\text{plus})} \quad (1)$$

where IC_{50} (minus) = IC_{50} determined from a 30-minute pre-incubation in the absence of NADPH and IC_{50} (plus) = IC_{50} determined from a 30-minute pre-incubation in the presence of NADPH.

2.3 | Efflux and solute carrier transporter inhibition

Treosulfan (concentrations up to 1000 μM) was tested as an inhibitor of the human transporters P-gp, BCRP, OATP1B1, OATP1B3, OAT1, OAT3, OCT2, OCT1, MATE1 and MATE2-K in various in vitro cell test systems, and of BSEP in membrane vesicles¹⁶ (unpublished data). Probe substrates loperamide (P-gp) and estrone 3-sulfate (BCRP), and the respective inhibitors cyclosporin A and novobiocin were incubated with the appropriate in vitro test system for a specific incubation time in the absence and presence of a range of concentrations of the test

compound treosulfan. The rate of transport of the probe substrate, which was used to determine apparent permeability (P_{app}) was calculated according to the equation given below:

$$P_{\text{app}} = \frac{\left(\frac{dQ}{dt}\right)}{A \times C_0} \quad (2)$$

where P_{app} is apparent permeability ($\text{cm/s} \times 10^{-6}$), dQ/dt is the rate of drug transport (pmol/s), A is the surface area of the membrane (cm^2) and C_0 is the initial donor concentration (nM, pmol/ cm^3). The individual replica P_{app} determined in the apical to basolateral direction was subtracted from the corresponding P_{app} determined in the basolateral to apical direction to give a transporter-mediated net secretory flux value. Each replicate's net secretory flux value was then converted to a percentage of the mean vehicle control transport activity, which was plotted against test compound concentration and subsequently fitted to calculate an IC_{50} value (concentration which produces 50% inhibition of vehicle control transport activity; Supporting Information Figure S15).

The positive inhibitor controls used for treosulfan SLC transporter assessment were rifamycin (OATP1B1), cyclosporin A (OATP1B3), probenecid (OAT1 and OAT3), verapamil (OCT2 and OCT1) and cimetidine (MATE1 and MATE2-K).

2.4 | PBPK model development

The PBPK analyses were performed using qualified installations of the PBPK software PK-Sim version 8.0 (<http://www.open-systems-pharmacology.org/>).¹⁷ The analytical approach is based on principles established in the European Medicines Agency (EMA) and/or FDA guidelines on the reporting of PBPK modeling and simulation (M&S).^{18,19} As the first step in model development, all available information on the drug regarding its ADME properties is gathered. This includes the drug-specific parameters used as input parameters and the characterisation of the organism or population.

2.5 | Treosulfan PBPK model development and qualification

Treosulfan is nonenzymatically, pH-dependently converted into its monoepoxide and diepoxide transformation products S,S-EDBM and S,S-DEB, respectively. This transformation process is systemic within all blood and tissue compartments. Treosulfan is excreted in the kidneys via glomerular filtration, and the fraction of unchanged treosulfan excreted in patients' urine is 15-40%.²⁰ No other transport or secretion processes in renal clearance are indicated. In the PBPK model, treosulfan transformation was implemented using a non-specific systemic enzymatic process (required in PK-Sim to implement transformation rates of any kind). The process was implemented such that the "enzyme" is "expressed" uniformly across all systemic compartments. The expression level was arbitrarily set to 1 $\mu\text{mol/L}$ (Figure 1). The reported glomerular filtration rate (GFR) of each

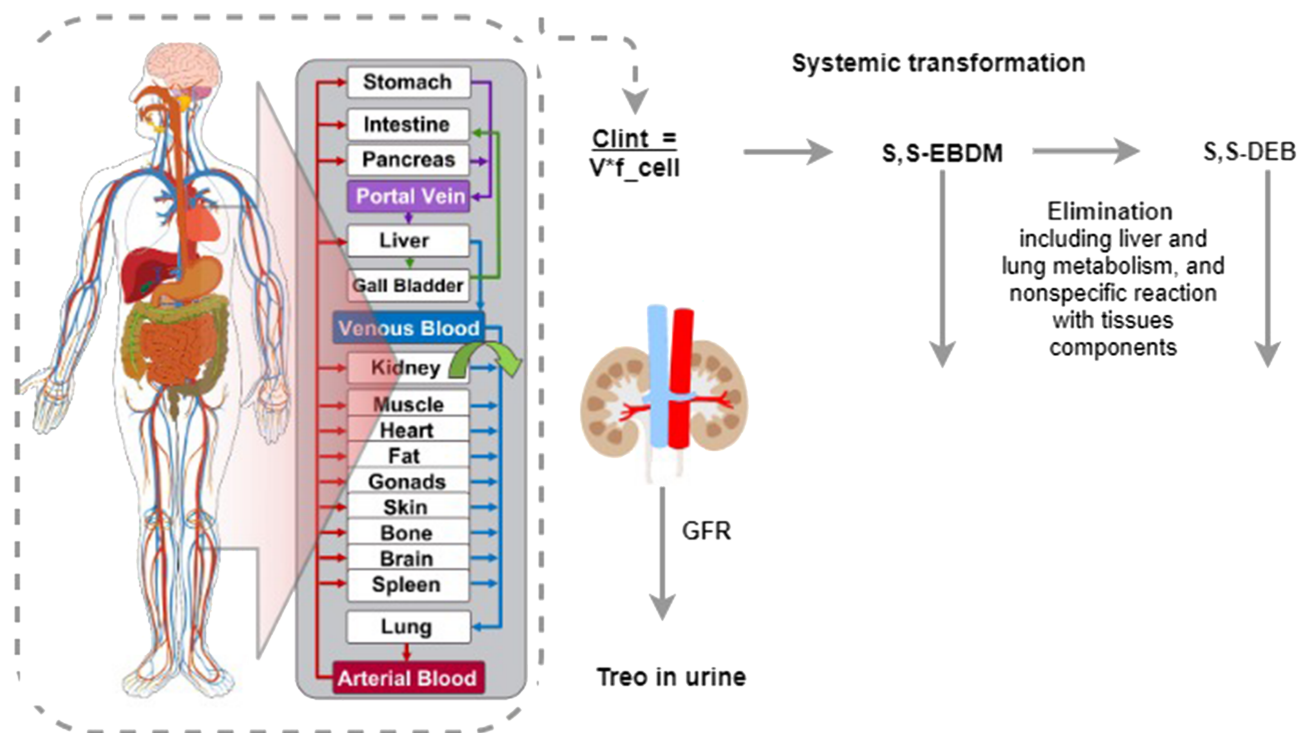


FIGURE 1 Physiologically-based pharmacokinetic model structure. Systemic chemical (nonenzymatic) transformation of treosulfan is implemented as a first-order process reaction rate in all physiological compartments. GFR, glomerular filtration rate; S,S-EBDM, (2S,3S)-1,2-epoxybutane-3,4-diol 4-methanesulfonate; S,S-DEB, (2S,3S)-1,2:3,4-diepoxybutane

patient was set according to their reported creatinine clearance (Supporting Information Table S1). The model was otherwise parameterized according to the parameters listed in Table 1, and the simulation was created using the partition coefficient and permeability calculation method PK-Sim Standard.

The PBPK model of treosulfan PKs was developed using individual data from study MC-FludT.14/L Part I (Supporting Information Table S1). For model development and qualification, study subjects were divided into two groups based on their administration protocol. Subjects which received an infusion exactly every 48 hours, as specified in the protocol, were taken into the qualification set and subjects for which the time of administration deviated from this exact timing were taken into the training set. This was done to receive a homogeneous set of concentration-time profiles for the qualification to be compared against a population simulation.

For the model development, a parameter identification (PI) routine was set up to characterise interindividual variability using the training data set. The PI was executed in PK-Sim using the Levenberg-Marquardt algorithm. Within the PI, the rate of systemic transformation and the fraction excreted via glomerular filtration were estimated (Supporting Information Table S1). From the individual resulting estimates, the mean and standard deviation were calculated for use as “User Defined Variability” in the population simulation for the model qualification using the qualification data set.

The qualification of the developed PBPK model of treosulfan consisted of a population simulation of 200 subjects using ranges for age,

gender, body weight and dosing information representative of the second half (qualification data set) of the study population. To evaluate the predictive performance of the PBPK model, the overall accuracy of the predicted PK parameters was assessed using the mean fold-error (MFE; the difference between predicted *in silico* and observed *in vivo* values from the qualification data set):

$$\text{MFE} = \frac{\text{PK parameter}_{\text{predicted mean}}}{\text{PK parameter}_{\text{observed mean}}} \quad (3)$$

The model was accepted when all predicted PK parameters were within 2-fold of the corresponding observed values (eg, MFE 0.5-2.0).²³

2.6 | PBPK DDI analyses with index substrates

The simulations required to analyse the DDIs of treosulfan with the selected FDA DDI index substrate drugs midazolam,^{24,25} digoxin^{24,26} and omeprazole^{27,28} were conducted in PK-Sim. The IC_{50} inhibition constants listed in Table 1 were used in the model to predict the reversible inhibitory potential of treosulfan as a competitive inhibitor.

The recalculation of the IC_{50} values to K_i values were conducted as outlined in Equation 4.^{29,30}

$$IC_{50} = (1 + [S] \times f_u / K_m) K_i \rightarrow K_i = IC_{50} / (1 + [S] \times f_u / K_m) \quad (4)$$

TABLE 1 Compound properties used as input parameters for the treosulfan PBPK model

Parameter	Value	Reference
MW (g/mol)	278.29	DrugBank
Compound type	Neutral	
Log $P_{O:W}$ (-)	-1.58	Literature ²⁰
f_u (-)	1	Literature ²⁰
B:P (-)	0.88	Literature ²¹
V_{ss} (L/kg or L)	17-34 L	Literature ²⁰
Transport		
Tubular reabsorption	...	Accounted for in estimated GFR fraction
Elimination		
CL_R (mL/min)	33 ± 6	Estimated (literature ²⁰ : 39 to 88)
GFR fraction (-)	0.95 ± 0.51	Estimated (literature ²⁰ : 0.41 ± 0.22)
DDI parameters		
IC_{50} CYP3A4 (μ M)	1870	Internal CYP inhibition assay (substrate: midazolam, 2.5 μ mol incubation)
K_i CYP3A4 (μ M)	1213	Calculated from IC_{50} and $f_{u, mic}$ (Equation 4; substrate: midazolam [$K_m = 2.73$])
$f_{u, mic}$ midazolam	0.55	Predicted by PK-Sim (0.5 mg/mL HLM)
IC_{50} CYP2C19 (μ M)	972	Internal CYP inhibition assay (substrate: mephenytoin, 25 μ mol incubation)
K_i CYP2C19 (μ M)	778	Calculated from IC_{50} and $f_{u, mic}$ (Equation 4; substrate: mephenytoin [$K_m = 100 \mu$ mol ²²])
$f_{u, mic}$ mephenytoin	0.98	Predicted by PK-Sim (0.5 mg/mL HLM)
IC_{50} P-gp (μ M)	3000	Internal CYP inhibition assay (substrate: loperamide, 25 μ mol incubation)
K_i P-gp (μ M)	1774.51	Calculated from IC_{50} and $f_{u, mic}$ (Equation 4; substrate: loperamide [$K_m = 36.2$; source: Cyprotex])
$f_{u, mic}$ loperamide	1	Assumed (worst-case scenario for DDI)
$f_{u, mic}$ treosulfan	1	Predicted by PK-Sim

Abbreviations: B:P, blood-plasma ratio; CL_R , renal clearance; F , bioavailability; f_u , fraction unbound in plasma; $f_{u, mic}$, fraction unbound in microsomal assay; GFR, glomerular filtration rate; HLM, human liver microsomes; IC_{50} , half maximal inhibitory concentration; K_i , inhibitor constant; K_m , Michaelis constant; $\log P$, lipophilicity; MW, molecular weight; V_{ss} , volume of distribution at steady state.

TABLE 2 Predicted variation in treosulfan pharmacokinetics for a variation in body size

Time	Mean	SD	CV%
2 hr	23.20	5.000	21.50
12 hr	0.54	0.051	9.44
24 hr	0.15	0.030	21.20

Note: Listed are the mean, standard deviation (SD) and coefficient of variation (CV%) for treosulfan pharmacokinetics in short (both thin and heavy) and tall (both thin and heavy) individuals, reflecting variation in body surface area. The corresponding simulated variability in pharmacokinetics is shown in Figure 3.

where IC_{50} is the half-maximal inhibitory concentration, $[S]$ is the (unbound) substrate concentration, K_m is the substrate concentration of half enzyme activity, K_i is the dissociation constant of the inhibitor-enzyme complex and f_u is the fraction unbound (from buffer or microsomal protein).

Requalification and DDI analysis of the adopted midazolam PBPK model as a substrate of CYP3A4: The published and qualified model for midazolam^{24,25} has been adopted for this analysis, and recreated and

resimulated to verify a correct model adoption. The simulations from the adopted model have been reproduced identically.

Requalification/verification of the adopted digoxin PBPK model as a substrate of P-gp: The published and qualified model for digoxin^{24,26} has been adopted for this analysis, and recreated and resimulated to verify a correct adaptation. The simulations from the adopted model have been reproduced identically.

Requalification/verification of the adopted omeprazole PBPK model as a substrate of CYP2C19: The published and qualified model for omeprazole^{27,28} has been adopted for this analysis, and recreated and resimulated to verify a correct adoption. The simulations from the adopted model have been reproduced identically.

2.7 | In silico DDI design

Simulations with mean representative individuals have been conducted to predict plasma concentrations and DDI AUC and C_{max} ratios for a single oral dose (2 mg) of midazolam or multiple oral doses (0.5 mg once-daily [QD]) of digoxin or multiple oral doses (20 mg QD)

of omeprazole in the absence of treosulfan and following the standard treosulfan conditioning treatment, where treosulfan is given as 2-hour intravenous infusions of either 10 or 14 g/m² on three consecutive days (total dose 30 or 42 g/m²).

2.8 | Nomenclature of targets and ligands

Key protein targets and ligands in this article are hyperlinked to corresponding entries in <http://www.guidetopharmacology.org>, the common portal for data from the IUPHAR/BPS Guide to PHARMACOLOGY, and are permanently archived in the Concise Guide to PHARMACOLOGY 2019/20.^{31,32}

3 | RESULTS

3.1 | Clinical data

Geometric mean profiles of treosulfan plasma concentrations were similar on day -6 and day -4. As was expected, the maximum concentrations were observed at the end of infusion after 2 hours. Model-independent pharmacokinetic parameters were calculated from plasma concentrations of treosulfan using noncompartmental procedures separately for day -6 and day -4. The observed C_{max} in the total population was slightly lower on day -4 (434.6 µg/mL [SD 17.5%]) than on day -6 (470.5 µg/mL [SD 18.5%]) in the total population. AUC was slightly higher on day -4 (1449 µg*h/mL [SD 17%]) than on day -6 (1424 µg*h/mL [SD 18%]). The apparent half-life was 1.86 hours (median, range 1.12 to 2.56 hours) on day -6 and 1.93 hours (median, range 1.51 to 3.83 hours) on day -4. Altogether, 294 urine samples were analysed for treosulfan. Urine samples were planned to be collected for 72 hours starting after the first treosulfan dose on day -6. However, several of the later samples are missing so that 10 patients were excluded from the pharmacokinetic evaluation of treosulfan urine concentrations on day -4, no patient was excluded on day -5 and two patients were excluded on day -6. About 40% of an administered dose was excreted in urine at 130.38 mL/min (coefficient of variation [CV%] = 31.98%).

3.2 | Nonclinical data

Treosulfan did not inhibit CYP1A2, CYP2B6, CYP2C8, CYP2C9, CYP2D6 or CYP3A4 using testosterone as the substrate under any of the pre-incubation conditions tested and therefore no IC_{50} or fold shift values were calculated.¹⁵ On the other hand, treosulfan returned a fold shift of 0.933 and 0.841 against CYP2C19 and CYP3A4 using midazolam as the substrate, respectively. Reversible IC_{50} values of 972 and 1870 µM for CYP2C19 and CYP3A4 were obtained using midazolam as the substrate, respectively.

The transporter inhibitory potential of treosulfan was assessed in various in vitro cell test systems and transporter-expressing

membrane vesicles to determine IC_{50} values.¹⁶ Under the assay conditions tested, treosulfan was determined to be an inhibitor of the probe substrate transport mediated via P-gp and MATE2-K, but not via OATP1B1, OATP1B3, OAT1, OAT3, OCT2, OCT1, MATE1 and BSEP. The IC_{50} value for P-gp inhibition was determined as 3000 µM. The IC_{50} value for MATE2-K inhibition was determined as 8210 µM (standard error of the fitted IC_{50} value = 1200 µM). As the observed $IC_{50} > >$ predicted C_{max} , MATE2-K inhibition was deemed as clinically not relevant. The corresponding K_i values as derived with Equation 4 are 1213 µM for CYP3A4, 972 µM for CYP2C19 and 1774.51 µM for P-gp (Table 1).

3.3 | PBPK model development and qualification

Parameter identification for the development of the treosulfan PBPK model for each patient in the training data set resulted in individual estimates for the rate of transformation of treosulfan and its renal clearance (Supporting Information Table S1). Both the pharmacokinetics of treosulfan and the amount of treosulfan excreted in the urine were captured well within the model and the simulated concentration-time profiles of all individual simulations from the training set are shown in Supporting Information Figures S1-S10. The use of measured creatinine clearance as an input parameter for the glomerular filtration rate did not predict renal excretion well, as estimates for GFR fraction in the model and measured creatinine clearance used as the baseline for the glomerular filtration rate are strongly negatively correlated ($r = -0.88$).

The population simulation for model qualification adding the mean and standard deviation from the individual resulting estimates for the rate of transformation and GFR fraction as “User Defined Variability” underpredicted renal clearance and slightly overpredicted PKs (Figure 2). Increasing mean GFR fraction by 70% in this group accurately predicts both renal excretion and PKs (data not shown), indicating a difference in baseline renal excretion but not in the transformation rate of treosulfan between the two groups (training vs qualification data set).

In a further investigation on variability, the PBPK model was used to assess changes in PK due to variations in physiology and GFR, as in a previous population PK (popPK) analysis of treosulfan PK,³³ body surface area (BSA) was identified as the major covariate but (measured) GFR was not. To assess the variability of treosulfan between individuals with strong differences in body size, the PBPK model was used to simulate treosulfan PK for a variation in body size in individuals with short (both thin and heavy) and tall (both thin and heavy) physique. Resulting changes in PK in the PBPK model were low for variations in body size but high for low values of GFR (GFR < 50% of baseline; Figure 3).

For all PBPK models the predicted and observed pharmacokinetic exposure parameters of midazolam, digoxin, omeprazole and treosulfan after ascending intravenous and oral doses in healthy adults and cancer populations are summarized in Figure 4. The simulated exposure parameters for all populations were consistent with the observed values. The MFE values for the AUC from time of the

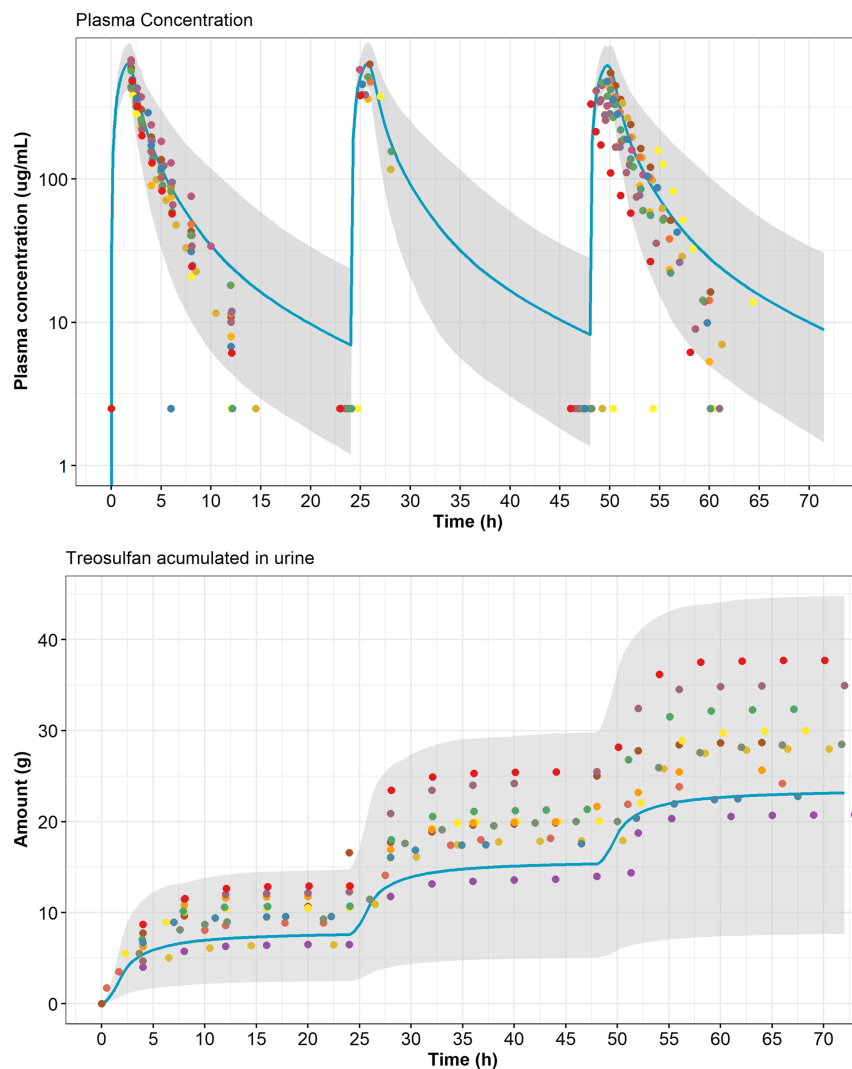


FIGURE 2 Population prediction of treosulfan pharmacokinetics during conditioning treatment following 2-h intravenous infusions of 14 g/m^2 on 3 consecutive days (total dose 42 g/m^2) using a population simulation ($n = 200$). The dots represent the individual observed data, the solid lines represent the simulated geometric mean and the shaded areas represent the 5th-95th percentile. Lower limit of quantification (LLOQ) for treosulfan measurements is $2.5 \text{ } \mu\text{g/mL}$

first dose to the last sampling time point ranged from 1.0 to 1.33 for midazolam, from 1.2 to 1.5 for digoxin, from 0.86 to 1.32 for omeprazole and from 1.33 to 1.53 for treosulfan. The MFE determined for C_{max} ranged from 1.5 to 1.8 for midazolam, from 1.1 to 1.6 for digoxin, from 1.0 to 1.5 for omeprazole and from 1.36 to 1.4 for treosulfan. The MFE values for AUC and C_{max} were well within 0.5 and 2 when comparing the observed and predicted exposure parameters and PK profiles for single and multiple doses (Figure 4).

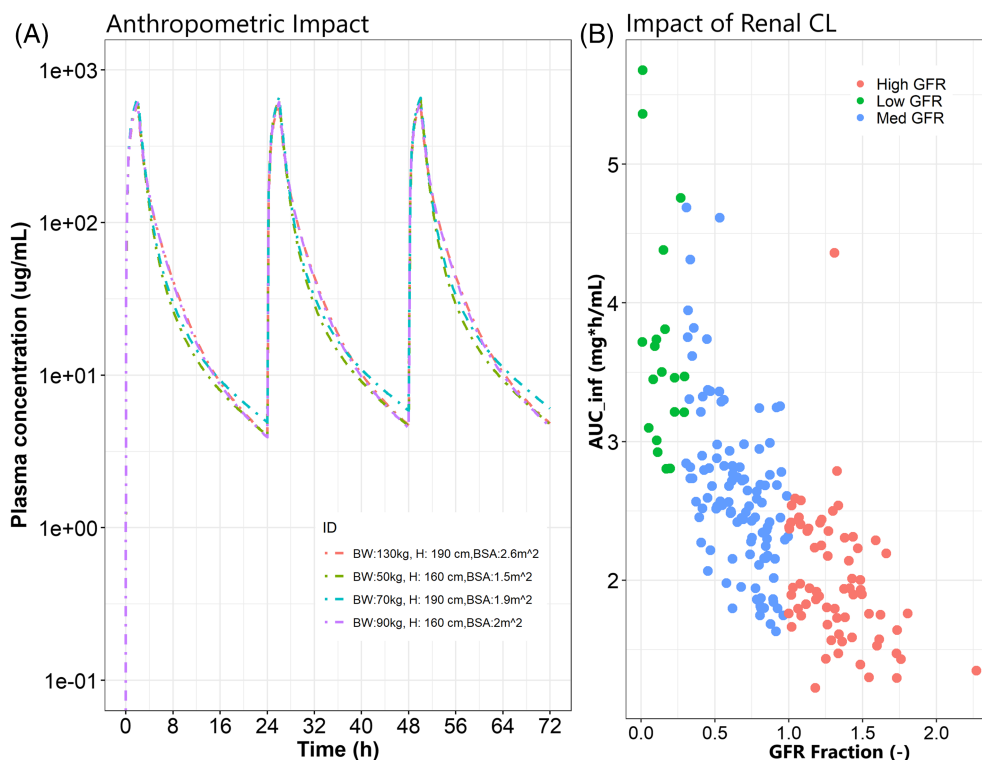
3.4 | Simulations of concentration-time profiles of DDI substrates

Simulations of the midazolam DDI scenario resulted in the AUC and C_{max} ratios as documented in Table 3 and depicted in Figure 5. Both C_{max} and AUC of midazolam were slightly increased during concurrent use of treosulfan. According to the predicted AUC and C_{max} ratios by the PBPK model, treosulfan can be classified as a weak inhibitor of CYP3A4 ($1.25 \leq \text{AUCR} < 2$). However, as concurrent use of drugs with the intravenous conditioning treatment is unlikely, it was

evaluated how the predicted DDI ratios change during concomitant use of a CYP3A4 substrate (ie, midazolam) in treosulfan conditioning treatment if the drugs are not given simultaneously. The effect of a time difference in dosing of midazolam of $-2, -1, +1, +2, +3, +4$ and $+8$ hours was evaluated with respect to the changes in the predicted DDI ratios (Table 4). The outcomes show a significant dependency of the DDI potential on dosing times. If midazolam is not given within 2 hours prior to or 8 hours after the 2-h intravenous treosulfan treatment, the DDI potential can be significantly decreased ($\text{AUCR} < 1.25$). The maximum AUCR for midazolam ($\text{AUCR} = 2.23$) is reached if the time difference in dosing of midazolam is $+1$ hour, dropping below a “moderate” interaction potential ($\text{AUCR} < 2$) when dosed concomitantly or 2 hours after treosulfan injection.

Simulations of the digoxin DDI scenario resulted in the AUC and C_{max} ratios as documented in Table 3 and depicted in Figure 5. Both C_{max} and AUC of digoxin did not increase during concurrent use of treosulfan. According to the predicted AUC and C_{max} ratios by the PBPK model, treosulfan likely cannot be classified as an inhibitor of P-gp ($\text{AUCR} < 1.25$). Given the predicted low interaction potential on P-gp substrates by treosulfan, no additional evaluations were conducted.

FIGURE 3 Predicted variation in treosulfan pharmacokinetics for a variation in body-size (A) and GFR fraction (B). The figure shows simulated curves for treosulfan pharmacokinetics (PK) in short (both thin and heavy) and tall (both thin and heavy) individuals, reflecting variation in body surface area. The calculated variability in PKs is shown in Table 2. The dose in each of the four cases was calculated as 14 g treosulfan/m² BSA. CL, clearance; GFR, glomerular filtration rate



Simulations of the omeprazole DDI scenario resulted in the AUC and C_{max} ratios documented in Table 3 and depicted in Figure 5. Both C_{max} and AUC of omeprazole were slightly increased during concurrent use of treosulfan. According to the predicted AUC and C_{max} ratios by the PBPK model, treosulfan can be classified as a weak inhibitor of CYP2C19 ($1.25 \leq AUCR < 2$). As for midazolam, the effect of a time difference in dosing of omeprazole of $-2, -1, +1, +2, +3, +4$ and $+8$ hours was evaluated with respect to the changes in the predicted DDI ratios. For omeprazole, the outcomes also show a significant dependency of the DDI potential on dosing times. If omeprazole is given within 2 hours prior to or 3 hours after the 2-hour intravenous treosulfan treatment, a significant (“weak”) interaction could be expected ($1.25 \leq AUCR < 2$ with maximum $AUCR = 1.60$), otherwise the potential for interaction is low.

4 | DISCUSSION

The final PBPK model for treosulfan, based on both in vitro and in vivo data, was able to generate plasma concentration-time profiles and exposure levels of treosulfan matching the treosulfan conditioning treatment of patients, where treosulfan is given as 2-hour intravenous infusions of 14 g/m² on 3 consecutive days (total dose 42 g/m²). The model was developed by optimising the systemic transformation rate and the GFR fraction to identify individual variability in the systemic transformation and renal clearance of treosulfan for model prediction and qualification. While model predictions for qualification were underpredicting drug PKs, this could be explained with the concomitant treatment with diuretics in the population used for

qualification or a higher volume of fluids administered to this group of hematopoietic stem cell transplantation (HSCT) patients possibly leading to a higher rate of renal clearance.²⁰ The general low variability of PKs across both anthropometric properties and GFR in patients without severe renal impairment may be used as a justification for a sparse sampling approach in future clinical analyses.

Patients enrolled across studies with treosulfan had either no or mild renal impairment or moderate impairment in rare cases. For patients with no or only mild renal impairment, the measured creatinine and derived observed renal clearance are not well correlated with renal excretion, and correlation is only significant for severe renal impairment.⁴³ Furthermore, concomitant use of diuretics during the study may further invalidate the a priori measured creatinine clearance values as valid input parameters for the PBPK model. Although the effects of diuretic use on GFR are transient and complex,⁴⁴ they might partly explain why the measured renal clearance is not a significant covariate in the popPK studies summarized in earlier simulation studies.²⁰ A further explanation could be high-volume fluid infusions in HSCT patients.²⁰

The model was used prospectively to predict the likely outcome of DDI with treosulfan during conditioning treatment as an inhibitor of CYP3A4, P-gp and CYP2C19 using midazolam, digoxin and omeprazole as corresponding substrates. The DDI scenarios were simulated using the developed PBPK model of treosulfan in combination with previously developed and published PBPK models of the substrates available as templates from the Open Systems Pharmacology (OSP) GitHub model template repositories.^{25–27} The recalculation of the IC_{50} values to K_i values resulted in K_i values of 1213 μ M for CYP3A4, 972 μ M for CYP2C19 and 1774.51 μ M for P-gp (Table 1). In

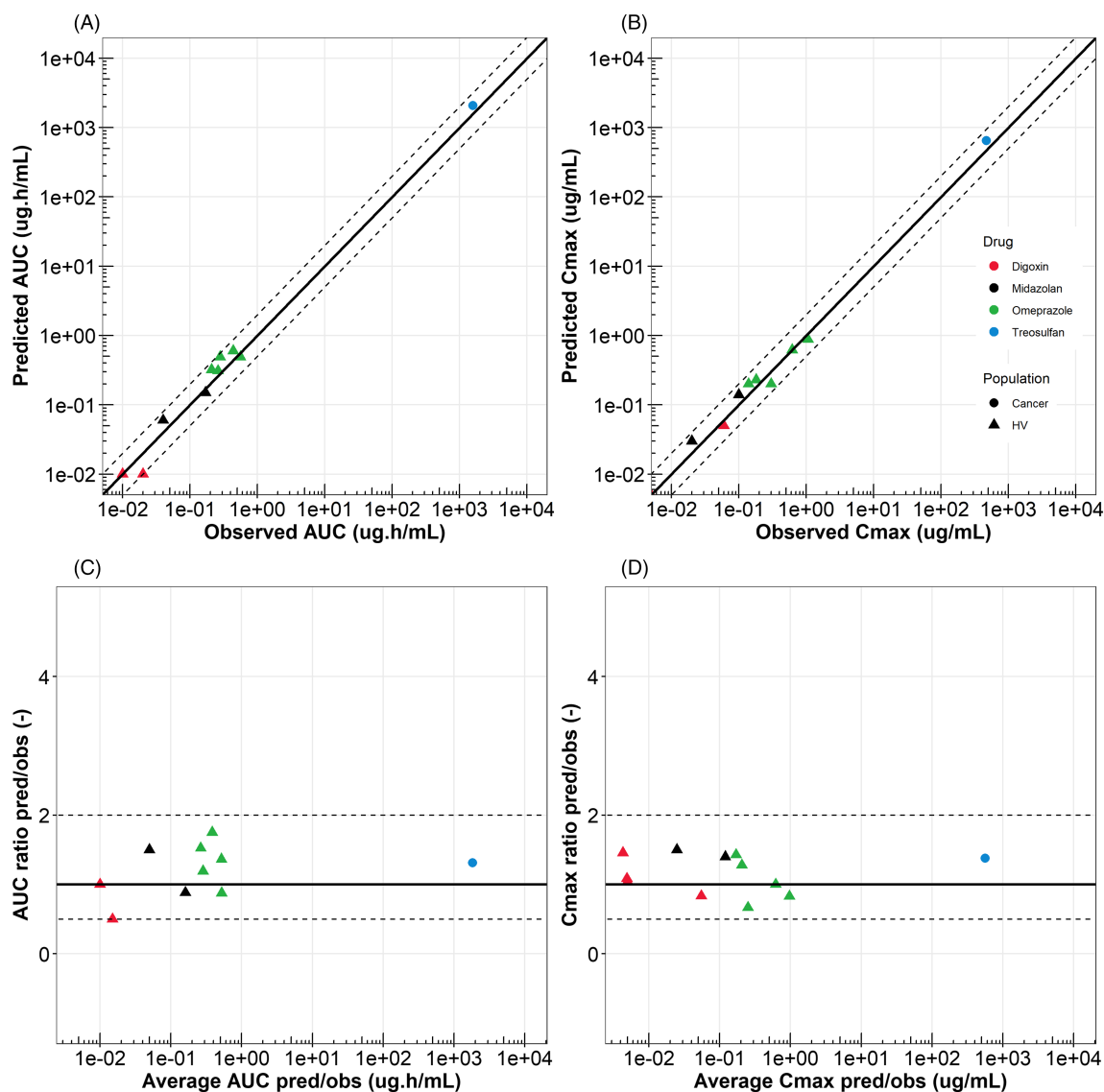


FIGURE 4 Comparison between simulated and observed pharmacokinetic parameters from several studies in the literature for different populations. (A) and (B) show the predicted vs observed. (C) and (D) show adaptations of a Bland-Altman plot where the y axis is plotted as the ratio (instead of the difference). Solid lines represent line of unity; dashed lines represent 2-fold difference. Literature data for the different compounds are digoxin: Greiner et al,³⁴ Kramer et al,³⁵ Hayward et al,³⁶ Oosterhuis et al³⁷ (extract, full qualification in evaluation report²⁶); midazolam: Smith et al,³⁸ Chung et al³⁹ (extract, full qualification in evaluation report²⁵); omeprazole: Andersson et al,^{40,41} Regardh et al⁴² (extract, full qualification in evaluation report²²). HV, healthy volunteers

Drug	Treosulfan dose	AUC ($\mu\text{mol}\cdot\text{min}/\text{l}$)	C_{max} ($\mu\text{mol}/\text{l}$)	AUC ratio	C_{max} ratio
Midazolam	None	4.18	0.028
	10 (g/m^2)	7.09	0.038	1.70	1.35
	14 (g/m^2)	8.14	0.041	1.95	1.46
Digoxin	None	6.67	7.73e-3
	10 (g/m^2)	7.04	8.38e-3	1.00	1.08
	14 (g/m^2)	7.32	8.86e-3	1.10	1.15
Omeprazole	None	100.0	0.66
	10 (g/m^2)	147.8	0.92	1.40	1.39
	14 (g/m^2)	160.8	0.99	1.60	1.50

TABLE 3 Predicted AUC and C_{max} values, and the calculated DDI AUC and C_{max} ratios for simultaneous dosing of a single oral dose of 2 mg of midazolam, daily oral dose of 20 mg of omeprazole and daily oral dose of 0.5 mg of digoxin in the absence of treosulfan and following the standard treosulfan conditioning treatment where treosulfan is given as 2-hour intravenous infusions of either 10 or 14 g/m^2 on 3 consecutive days (total dose 30 or 42 g/m^2)

conclusion, the DDI analysis with sensitive index substrates midazolam, digoxin and omeprazole for CYP3A4, P-gp and CYP2C19 predicted a weak ($1.25 \leq \text{AUCR} < 2$) to moderate ($2 \leq \text{AUCR} < 5$) interaction for CYP3A4, a weak interaction for CYP2C19 and a negligible ($\text{AUCR} < 1.25$) interaction for P-gp.

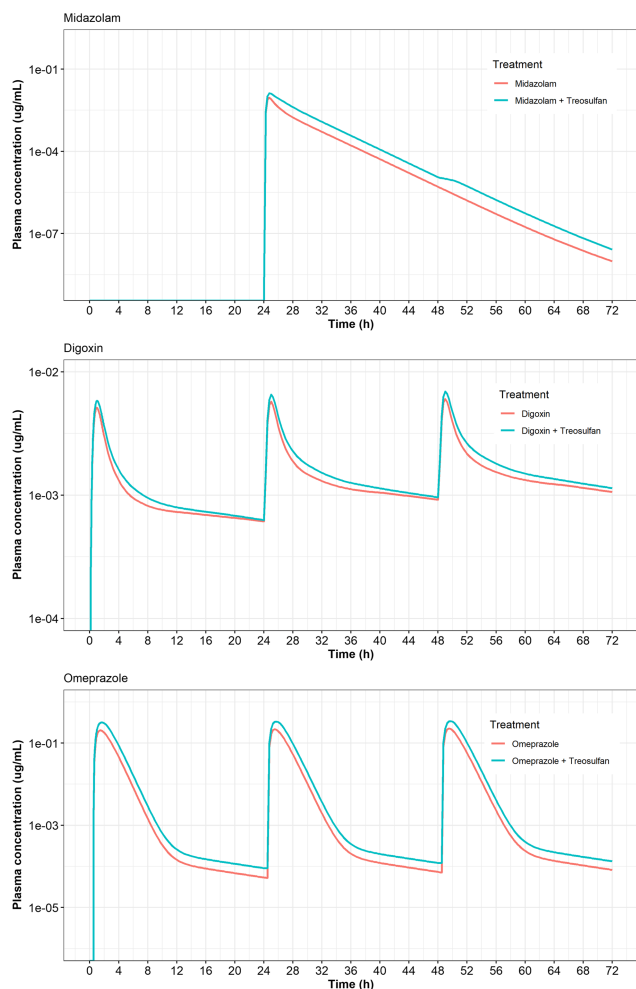


FIGURE 5 Predicted plasma concentrations of probe substrate of CYP3A4 (midazolam), CYP2C19 (omeprazole) and P-gp (digoxin) after multiple oral doses in the absence of treosulfan (red line) and following the standard treosulfan conditioning treatment (blue line) where treosulfan is given as 2-hour intravenous infusions of 14 g/m^2 on 3 consecutive days (total dose 42 g/m^2). The corresponding AUC and C_{max}

Clinical PK data used for PBPK modelling originated from adult patients treated with a 2-hour infusion of 14 g/m^2 treosulfan. Meanwhile, the approved treosulfan conditioning schedule has been modified for adult patients with malignant diseases. The recommended treosulfan dose for these patients has been reduced to $3 \times 10 \text{ g/m}^2$, postponing the start of treatment to day -4 prior to allogeneic HSCT.⁴⁵ The modified dose and treatment regimen resulted from the observation of a significantly prolonged duration of neutropenia and inherent serious infectious complications in the initial treosulfan arm compared with the reference arm in the pivotal randomized phase III study MC-FludT.14/L Part I.¹⁴ The difference in duration of neutropenia between the two study arms, however, can be predominantly attributed to the fact that the treosulfan conditioning treatment started 2 days earlier (on day -6) than the intensity-reduced busulfan reference treatment (on day -4). After modification of the treosulfan dose and application schedule (MC-FludT.14/L Part II),^{14,46} the duration of neutropenia was still significantly longer in the treosulfan arm compared with the reference arm (median difference of 1.5 days). This difference most probably reflects the earlier demonstrable effect of the higher myelotoxic potential even of the reduced treosulfan dose compared with the intensity-reduced busulfan reference treatment and—to a lesser extent—dose-dependent myelotoxic properties of the two treosulfan doses. This is also verified by the steeper decline of neutrophil counts after treosulfan treatment, whereas the time to neutrophil regeneration after allogeneic transplant was identical in both study arms. Finally, the modified (“reduced toxicity”) treosulfan treatment regimen resulted in a significant reduction of nonrelapse mortality without increased incidence of relapse or progression after allogeneic transplantation, while acute nonhaematological organ toxicities were comparable between the two treatment arms. However, in case of malignant paediatric or nonmalignant transplant indications in children and adults, intensified conditioning regimens, including treosulfan exposure to $3 \times 14 \text{ g/m}^2$, are frequently applied.^{47–49} Irrespective of the reduced treosulfan dose of 10 g/m^2 recommended for older and comorbid adult AML and MDS patients, and a correspondingly diminished potential for DDI, the PBPK-based analysis still predicts a weak inhibitor potential ($1.25 \leq \text{AUCR} < 2$) for treosulfan with both CYP3A4 and CYP2C19.

The risk for DDI varies depending on the timing of concomitant dosing. The maximum AUCR for midazolam ($\text{AUCR} = 2.23$) is reached if the time difference in dosing of midazolam is $+1$ hour,

TABLE 4 Predicted drug-drug interaction (DDI) AUC and C_{max} ratios for a single simultaneous and time-shifted oral doses of 2 mg of midazolam and 20 mg of omeprazole during the standard treosulfan conditioning treatment

Drug	DDI ratio	Time of administration							
		-2 h	-1 h	Simultaneous	$+1 \text{ h}$	$+2 \text{ h}$	$+3 \text{ h}$	$+4 \text{ h}$	$+8 \text{ h}$
Midazolam	AUC ratio (–)	1.22	1.34	1.95	2.23	1.96	1.65	1.48	1.22
	C_{max} ratio (–)	1.03	1.03	1.46	1.80	1.73	1.50	1.37	1.17
Omeprazole	AUC ratio (–)	1.24	1.46	1.60	1.49	1.30	1.19	1.14	1.10
	C_{max} ratio (–)	1.00	1.23	1.50	1.48	1.29	1.18	1.12	1.09

Note. Treosulfan is given as 2-h intravenous infusions of 14 g/m^2 on 3 consecutive days (total dose 30 or 42 g/m^2).

dropping below a “moderate” interaction potential ($AUCR < 2$) when dosed concomitantly or 2 hours after treosulfan injection. If omeprazole is given within 2 hours prior to or 3 hours after the 2-hour intravenous treosulfan treatment, a significant (“weak”) interaction could be expected ($1.25 \leq AUCR < 2$, with maximum $AUCR = 1.60$), otherwise the potential for interaction is low. The interaction potential can be reduced to “no interaction” ($AUCR < 1.25$) if the concomitantly used drugs tested in our model are dosed 2 hours before or 8 hours after the 2-hour intravenous infusion of treosulfan. To minimise risk, however, medicinal products with a narrow therapeutic index (eg, carbamazepine and dofetilide) that are substrates for CYP3A4 and CYP2C19 should be carefully considered and monitored during treatment with treosulfan. However, it has to be considered that the potential for DDIs after treosulfan infusion is rather limited compared to, for example, busulfan,⁵⁰ supporting the generally reported excellent tolerability of treosulfan-based conditioning treatment.

5 | CONCLUSION

Due to a potentially weak DDI, medicinal products with a narrow therapeutic index that are substrates for CYP3A4 and CYP2C19 should be carefully considered and monitored when administered simultaneously with treosulfan-based conditioning therapy. Considering the complexity of conditioning treatment and the respective PK properties of the concomitantly used drugs (eg, half-life), theoretically the interaction potential on all evaluated mechanisms can be reduced to “no interaction” ($AUCR < 1.25$) in the case where concomitantly used drugs are dosed 2 hours before or 8 hours after the 2-hour intravenous infusion during the treosulfan conditioning treatment.

ACKNOWLEDGEMENTS

This work was funded by medac GmbH. The software OSP Suite (PBPK software PK-Sim[®] and MoBi[®]) is a managed and quality-assured open-source and open-access project, and the software is freely available to all users from academia and industry alike.

COMPETING INTERESTS

S.S., F.S.M. and P.B. are employees of esqLABS GmbH, the contract research organization (CRO) contracted by medac for this work. D.W. B. and R.A.H. report no conflict of interest. S.B., J.B. and C.H. are employees of medac GmbH, and A.R. was an employee of medac GmbH at the time of the investigation.






CONTRIBUTORS

S.S., J.B., C.H., S.B. and A.R. designed the research. D.W.B. and R.A.H. provided the clinical PK data of clinical trial MC-FludT.14/L Part I. S.S. developed the PBPK model and algorithms. S.S., P.B. and F.S.M. developed the compound files, ran simulations and analysed the data. All authors wrote, reviewed and approved the final manuscript.

DATA AVAILABILITY STATEMENT

PBPK models for midazolam, digoxin and omeprazole are available on <https://github.com/Open-Systems-Pharmacology/OSP-PBPK-Model-Library>.

ORCID

Stephan Schaller  <https://orcid.org/0000-0003-1046-7651>
 Frederico S. Martins  <https://orcid.org/0000-0001-5555-8771>
 Pavel Balazki  <https://orcid.org/0000-0002-8199-9869>
 Sonja Böhm  <https://orcid.org/0000-0003-4214-1816>
 Joachim Baumgart  <https://orcid.org/0000-0003-4502-2847>
 Dietrich W. Beelen  <https://orcid.org/0000-0001-5050-220X>
 Arne Ring  <https://orcid.org/0000-0002-4324-5820>

REFERENCES

- Public Health – European Commission. Union Register of medicinal products. Accessed September 5, 2020. <https://ec.europa.eu/health/documents/community-register/html/h1351.htm>
- Sehouli J, Tomè O, Dimitrova D, et al. A phase III, open label, randomized multicenter controlled trial of oral versus intravenous treosulfan in heavily pretreated recurrent ovarian cancer: a study of the North-Eastern German Society of Gynecological Oncology (NOGGO). *J Cancer Res Clin Oncol*. 2017;143(3):541-550. <https://doi.org/10.1007/s00432-016-2307-0>
- Romański M, Pogorzelska A, Główna FK. Kinetics of in vitro guanine-N7-alkylation in calf thymus DNA by (2S,3S)-1,2-epoxybutane-3,4-diol 4-methanesulfonate and (2S,3S)-1,2:3,4-diepoxybutane: Revision of the mechanism of DNA cross-linking by the prodrug treosulfan. *Mol Pharm*. 2019;16(6):2708-2718. <https://doi.org/10.1021/acs.molpharmaceut.9b00251>
- Scheulen ME, Hilger RA, Oberhoff C, et al. Clinical phase I dose escalation and pharmacokinetic study of high-dose chemotherapy with treosulfan and autologous peripheral blood stem cell transplantation in patients with advanced malignancies. *Clin Cancer Res*. 2000;6:4209-4216.
- Gherezghiher TB, Ming X, Villalta PW, Campbell C, Tretyakova NY. 1,2,3,4-diepoxybutane-induced DNA-protein cross-linking in human fibrosarcoma (HT1080) cells. *J Proteome Res*. 2013;12(5):2151-2164. <https://doi.org/10.1021/pr3011974>
- Michaelson-Richie ED, Loeber RL, Codreanu SG, et al. DNA-protein cross-linking by 1,2,3,4-diepoxybutane. *J Proteome Res*. 2010;9(9):4356-4367. <https://doi.org/10.1021/pr1000835>
- Waters NJ. Evaluation of drug-drug interactions for oncology therapies: *in vitro-in vivo* extrapolation model-based risk assessment: *In vitro-in vivo* model-based risk assessment of DDI in oncology. *Br J Clin Pharmacol*. 2015;79(6):946-958. <https://doi.org/10.1111/bcp.12563>
- Jansman FGA, Reyners AKL, van Roon EN, et al. Consensus-based evaluation of clinical significance and management of anticancer drug interactions. *Clin Ther*. 2011;33(3):305-314. <https://doi.org/10.1016/j.clinthera.2011.01.022>
- Buajordet I, Ebbesen J, Erikssen J, Brørs O, Hilberg T. Fatal adverse drug events: the paradox of drug treatment. *J Intern Med*. 2008;250(4):327-341. <https://doi.org/10.1111/j.1365-2796.2001.00892.x>
- Gerlowski LE, Jain RK. Physiologically based pharmacokinetic modeling: principles and applications. *J Pharm Sci*. 1983;72(10):1103-1127. <https://doi.org/10.1002/jps.2600721003>
- Jones HM, Gardner IB, Watson KJ. Modelling and PBPK simulation in drug discovery. *AAPS J*. 2009;11(1):155-166. <https://doi.org/10.1208/s12248-009-9088-1>
- Kuepfer L, Niederalt C, Wendl T, et al. Applied concepts in pbpk modeling: How to build a PBPK/PD model. *CPT Pharmacometrics*

- Syst Pharmacol.* 2016;5(10):516-531. <https://doi.org/10.1002/psp4.12134>
13. Dallmann A, Solodenko J, Ince I, Eissing T. Applied concepts in PBPK modeling: How to extend an open systems pharmacology model to the special population of pregnant women. *CPT Pharmacometrics Syst Pharmacol* Published online March. 2018;23(7):419-431. <https://doi.org/10.1002/psp4.12300>
 14. Clinical Phase III Trial to Compare Treosulfan-based Conditioning Therapy With Busulfan-based Reduced-intensity Conditioning (RIC) Prior to Allogeneic Haematopoietic Stem Cell Transplantation in Patients With AML or MDS Considered Ineligible to Standard Conditioning Regimens. Published online December 1, 2010. https://www.clinicaltrialsregister.eu/ctr-search/search?query=eudract_number:2008-002356-18
 15. CYP1269 R9. Study to Investigate the Cytochrome P450 Time Dependent Inhibition (IC50 Shift) Potential of the Test Compound, Treosulfan. medac contracted report; 2018.
 16. CYP1269 R9. Study to Investigate Whether Compound Treosulfan Is an Inhibitor of the Human Transporters P-Gp, BCRP, OATP1B1, OATP1B3, OAT1, OAT3, OCT2, OCT1, MATE1, MATE2-K and BSEP in Various in Vitro Test Systems. medac contracted report; 2018.
 17. Lippert J, Burghaus R, Edginton A, et al. Open systems pharmacology community—An open access, open source, open science approach to modeling and simulation in pharmaceutical sciences. *CPT Pharmacometrics Syst. Pharmacol.* 2019;8(12):878-882. <https://doi.org/10.1002/psp4.12473>
 18. EMA. Guideline on the qualification and reporting of physiologically based pharmacokinetic (PBPK) modelling and simulation. http://www.ema.europa.eu/docs/en_GB/document_library/Scientific_guideline/2016/07/WC500211315.pdf
 19. FDA CDER. Physiologically Based Pharmacokinetic Analyses – Format and Content Guidance for Industry. U.S. Food and Drug Administration. Published October 18, 2019. Accessed November 19, 2019. <http://www.fda.gov/regulatory-information/search-fda-guidance-documents/physiologically-based-pharmacokinetic-analyses-format-and-content-guidance-industry>
 20. Romański M, Wachowiak J, Główska FK. Treosulfan pharmacokinetics and its variability in pediatric and adult patients undergoing conditioning prior to hematopoietic stem cell transplantation: Current state of the art, in-depth analysis, and perspectives. *Clin Pharmacokinet.* 2018;57(10):1255-1265. <https://doi.org/10.1007/s40262-018-0647-4>
 21. Romański M, Zacharzewska A, Teżyk A, Główska FK. In vivo red blood cells/plasma partition coefficient of treosulfan and its active monooxide in rats. *Eur J Drug Metab Pharmacokinet.* 2018;43(5):565-571. <https://doi.org/10.1007/s13318-018-0469-7>
 22. Shirasaka Y, Chaudhry AS, McDonald M, et al. Interindividual variability of CYP2C19-catalyzed drug metabolism due to differences in gene diplotypes and cytochrome P450 oxidoreductase content. *Pharmacogenomics J.* 2016;16(4):375-387. <https://doi.org/10.1038/tpj.2015.58>
 23. Martins FS, Zhu P, Heinrichs MT, Sy SKB. Physiologically-based pharmacokinetic-pharmacodynamic evaluation of meropenem plus fosfomycin in pediatrics. *Br J Clin Pharmacol* Published online July 7, 2020:bcp.14456. 87(3):1012-1023. <https://doi.org/10.1111/bcp.14456>
 24. Hanke N, Frechen S, Moj D, et al. PBPK models for CYP3A4 and P-gp DDI prediction: A modeling network of rifampicin, itraconazole, clarithromycin, midazolam, alfentanil, and digoxin. *CPT Pharmacometrics Syst Pharmacol.* 2018;7(10):647-659. <https://doi.org/10.1002/psp4.12343>
 25. Open-Systems-Pharmacology/Midazolam-Model. Open Systems Pharmacology; 2020. Accessed July 28, 2020. <https://github.com/Open-Systems-Pharmacology/Midazolam-Model>
 26. Open-Systems-Pharmacology/Digoxin-Model. Open Systems Pharmacology; 2019. Accessed July 28, 2020. <https://github.com/Open-Systems-Pharmacology/Digoxin-Model>
 27. Open-Systems-Pharmacology/Omeprazole-Model. Open Systems Pharmacology; 2020. Accessed August 24, 2020. <https://github.com/Open-Systems-Pharmacology/Omeprazole-Model>
 28. Kanacher T, Lindauer A, Mezzalana E. A Physiologically-Based Pharmacokinetic (PBPK) Model Network for the Prediction of CYP1A2 and CYP2C19 Drug-Drug-Gene Interactions with Fluvoxamine, Omeprazole, S-mephenytoin, Moclobemide, Tizanidine, Mexiletine, Ethinylestradiol, and Caffeine. *Pharmaceutics.* 2020;12(12):1191. <https://doi.org/10.3390/pharmaceutics12121191>
 29. Brandt RB, Laux JE, Yates SW. Calculation of inhibitor K_i and inhibitor type from the concentration of inhibitor for 50% inhibition for Michaelis-Menten enzymes. *Biochem Med Metab Biol.* 1987;37(3):344-349. [https://doi.org/10.1016/0885-4505\(87\)90046-6](https://doi.org/10.1016/0885-4505(87)90046-6)
 30. Cer RZ, Mudunuri U, Stephens R, Lebeda FJ. IC50-to-Ki: a web-based tool for converting IC50 to K_i values for inhibitors of enzyme activity and ligand binding. *Nucleic Acids Res.* 2009;37(Web Server issue):W441-W445. <https://doi.org/10.1093/nar/gkp253>
 31. Alexander SPH, Fabbro D, Kelly E, et al. THE CONCISE GUIDE TO PHARMACOLOGY 2019/20: Enzymes. *Br J Pharmacol.* 2019;176(S1):S297-S396. <https://doi.org/10.1111/bph.14752>
 32. Alexander SPH, Kelly E, Mathie A, et al. THE CONCISE GUIDE TO PHARMACOLOGY 2019/20: Transporters. *Br J Pharmacol.* 2019;176(S1):S397-S493. <https://doi.org/10.1111/bph.14753>
 33. Reijmers T. Population PK-modelling of treosulfan in paediatric allogeneic transplant patients. Poster presented at the: Population Approach Group in Europe; January 6, 2018; Montreux, Switzerland. <https://www.page-meeting.org/default.asp?id=42&keuze=meeting>
 34. Greiner B, Eichelbaum M, Fritz P, et al. The role of intestinal P-glycoprotein in the interaction of digoxin and rifampin. *J Clin Invest.* 1999;104(2):147-153.
 35. Kramer WG, Kolibash AJ, Lewis RP, Bathala MS, Visconti JA, Reaming RH. Pharmacokinetics of digoxin: Relationship between response intensity and predicted compartmental drug levels in man. *J Pharmacokinet Biopharm.* 1979;7(1):47-61. <https://doi.org/10.1007/BF01059440>
 36. Hayward RP, Greenwood H, Hamer J. Comparison of digoxin and medigoxin in normal subjects. *Br J Clin Pharmacol.* 1978;6(1):81-86.
 37. Oosterhuis B, Jonkman JH, Andersson T, Zuiderwijk PB, Jedema JN. Minor effect of multiple dose omeprazole on the pharmacokinetics of digoxin after a single oral dose. *Br J Clin Pharmacol.* 1991;32(5):569-572. <https://doi.org/10.1111/j.1365-2125.1991.tb03953.x>
 38. Smith MT, Eadie MJ, Brophy TO. The pharmacokinetics of midazolam in man. *Eur J Clin Pharmacol.* 1981;19(4):271-278. <https://doi.org/10.1007/BF00562804>
 39. Chung E, Nafziger AN, Kazierad DJ, Bertino JS. Comparison of midazolam and simvastatin as cytochrome P450 3A probes. *Clinical Pharmacol Therapeutics.* 2006;79(4):350-361. <https://doi.org/10.1016/j.clpt.2005.11.016>
 40. Andersson T, Cederberg C, Heggelund A, Lundborg P. The pharmacokinetics of single and repeated once-daily doses of 10, 20 and 40mg omeprazole as enteric-coated granules. *Drug Invest.* 1991;3(1):45-52. <https://doi.org/10.1007/BF03259540>
 41. Andersson T, Holmberg J, Röhs K, Walan A. Pharmacokinetics and effect on caffeine metabolism of the proton pump inhibitors, omeprazole, lansoprazole, and pantoprazole. *Br J Clin Pharmacol.* 1998;45(4):369-375. <https://doi.org/10.1046/j.1365-2125.1998.t01-1-00702.x>
 42. Regårdh CG, Andersson T, Lagerström PO, Lundborg P, Skånberg I. The pharmacokinetics of omeprazole in humans – a study of single

- intravenous and oral doses. *Ther Drug Monit.* 1990;12(2):163-172. <https://doi.org/10.1097/00007691-199003000-00010>
43. Levey AS, Stevens LA, Schmid CH, et al. A new equation to estimate glomerular filtration rate. *Ann Intern Med.* 2009;150(9):604-612. <https://doi.org/10.7326/0003-4819-150-9-200905050-00006>
44. Huang X, Dorhout Mees E, Vos P, Hamza S, Braam B. Everything we always wanted to know about furosemide but were afraid to ask. *Am J Physiol Renal Physiol.* 2016;310(10):F958-F971. <https://doi.org/10.1152/ajprenal.00476.2015>
45. Union Register of medicinal products for human use. Published online June 20, 2019. <https://ec.europa.eu/health/documents/community-register/html/h1351.htm>
46. Beelen DW, Trenschele R, Stelljes M, et al. Treosulfan or busulfan plus fludarabine as conditioning treatment before allogeneic haemopoietic stem cell transplantation for older patients with acute myeloid leukaemia or myelodysplastic syndrome (MC-FludT.14/L): a randomised, non-inferiority, phase 3 trial. *Lancet Haematol.* 2020;7(1):e28-e39. [https://doi.org/10.1016/S2352-3026\(19\)30157-7](https://doi.org/10.1016/S2352-3026(19)30157-7)
47. Kalwak K, Mielcarek M, Patrick K, et al. Treosulfan-fludarabine-thiotepa-based conditioning treatment before allogeneic hematopoietic stem cell transplantation for pediatric patients with hematological malignancies. *Bone Marrow Transplant.* 2020;55(10):1996-2007. <https://doi.org/10.1038/s41409-020-0869-6>
48. Burroughs LM, Nemecek ER, Torgerson TR, et al. Treosulfan-based conditioning and hematopoietic cell transplantation for nonmalignant diseases: a prospective multicenter trial. *Biol Blood Marrow Transplant.* 2014;20(12):1996-2003. <https://doi.org/10.1016/j.bbmt.2014.08.020>
49. Slatter MA, Rao K, Abd Hamid IJ, et al. Treosulfan and fludarabine conditioning for hematopoietic stem cell transplantation in children with primary immunodeficiency: UK experience. *Biol Blood Marrow Transplant.* 2018;24(3):529-536. <https://doi.org/10.1016/j.bbmt.2017.11.009>
50. Myers AL, Kawedia JD, Champlin RE, et al. Clarifying busulfan metabolism and drug interactions to support new therapeutic drug monitoring strategies: a comprehensive review. *Expert Opin Drug Metab Toxicol.* 2017;13(9):901-923. <https://doi.org/10.1080/17425255.2017.1360277>

SUPPORTING INFORMATION

Additional supporting information may be found in the online version of the article at the publisher's website.

How to cite this article: Schaller S, Martins FS, Balazki P, et al. Evaluation of the drug-drug interaction potential of treosulfan using a physiologically-based pharmacokinetic modelling approach. *Br J Clin Pharmacol.* 2022;88(4):1722-1734. doi: 10.1111/bcp.15081